Edelweiss Applied Science and Technology
ISSN: 2576-8484
Vol. 9, No. 9, 1367-1376
2025
Publisher: Learning Gate
DOI: 10.55214/2576-8484.v9i9.10135

Non-isothermal crystallization kinetics of epoxidized soybean oil on poly (Lactic acid) stereocomplexes

Wenwei Li[1,2], Xiangli Lu[1], Zhiqiao Kuang[1], Zhiyong Yan[1*]
[1]College of Mechanical Engineering, Hunan Mechanical & Electrical Polytechnic, Changsha 410151, Hunan, China; liwenwei918@gmail.com (W.L.) 404939913@qq.com (X.L.) 31733926@qq.com (Z.K.) 122198956@qq.com (Z.Y.)
[2]Manufacturing and Materials Research Unit, Department of Manufacturing Engineering, Faculty of Engineering, Mahasarakham University, Mahasarakham 44150, Thailand.

Abstract: The crystallization of polylactic acid (PLA) stereocomposites is an effective approach to enhance the mechanical and thermal properties of PLA materials, while epoxidized soybean oil (ESO) has been demonstrated to exhibit good compatibility with PLA. This study prepared composite samples of PLA stereocomposites with ESO via solution blending. The non-isothermal crystallization kinetics of PLA blends were determined using the Jeziorny and Mo methods. Results indicate that the Kc value of SC-PLA-ESO increases with cooling rate, demonstrating accelerated polymer crystallization at higher cooling rates. The non-isothermal crystallization kinetics of PLA blends were investigated using the Jeziorny and Mo methods. Results showed that the Kc value of the SC-PLA-ESO system increased with cooling rate, indicating that the polymer crystallization rate is proportional to the cooling rate. simultaneously, the increase in F(T) values for ESO-containing blends at identical relative crystallinity indicates that ESO enhances the crystallization rate of PLA blends. This conclusion significantly enriches the crystallography theory of PLA.

Keywords: *Crystallization kinetics, ESO, PLA.*

1. Introduction

Polylactic acid (PLA) has biodegradable properties, allowing it to slowly decompose in natural environments and thereby avoiding environmental pollution. It is primarily made from starch-rich agricultural products such as corn, wheat, and sugar beets [1-3] produced through biotechnological synthesis. Unlike traditional plastic materials, PLA does not rely on petroleum-based chemicals, meaning it does not contain harmful heavy metals or other substances. During both production and use, PLA poses no negative impact on the environment or human health, ensuring its high level of safety [4-6]. The environmental friendliness of PLA is not only reflected in its biodegradability but also in the sustainability of its raw material sources. Using renewable agricultural products as raw materials reduces dependence on finite resources and minimizes environmental damage.

From an application perspective, PLA demonstrates unique advantages in food packaging materials due to its biodegradability and environmental friendliness [7]. However, the main obstacles to PLA's future development in high-temperature applications are its low melting temperature and poor toughness, which are caused by its low crystallinity and sluggish crystallization rate [8, 9]. The poor crystallization ability of PLA directly affects its toughness and heat resistance performance. Therefore, current research on PLA materials primarily focuses on enhancing its crystallization performance to improve its performance during use [10, 11].

The most common and effective method for enhancing PLA materials is to utilize the enantiomeric structure of L-PLA and D-PLA to form stereocomplex crystals [12]. These crystals can be produced in both molten and solution states. Stereocomplex crystals are a unique type of polycrystal characterized

History: Received: 7 July 2025; Revised: 19 August 2025; Accepted: 22 August 2025; Published: 22 September 2025
* Correspondence: 122198956@qq.com

by strong intermolecular hydrogen bonding interactions [13, 14] which can increase the melting temperature of PLA materials by over 50°C.

Epoxidized soybean oil (ESO) is a common green plasticizer. From a molecular structural perspective, epoxidized soybean oil contains epoxy groups and flexible long chains, making it suitable as a plasticizer for polymers [15, 16]. It has also been demonstrated to have good compatibility with polylactic acid. The flexible ESO interface layer designed by Ren, et al. [17] promotes effective energy dissipation and stress dispersion during stress transfer, effectively solving the problem of insufficient toughness in traditional PLA materials. Zhang, et al. [18] obtained a composite material with a high tensile strength of 52.8 MPa by adding 10% ESO and 3% DOPO. The fracture elongation and impact strength were 26.3 times and 67.5% higher than those of PLA. Additionally, the material demonstrated greatly improved UV protection and soil degradation performance while maintaining excellent thermal stability. Ge and Dou [19] verified that the combination of ESO and 4370 S produced ultra-tough PLA biocomposites with notched impact strength above 300% and fracture elongation over 300%, respectively.

Crystallization kinetics primarily investigates the formation mechanisms and processes of crystallization in polymeric materials, as well as the interrelationship between crystallization temperature and time on crystallinity and crystallization rate. The impact of varying ESO concentrations on the crystallization behavior of SC-PLA blends was investigated. SC-PLA-ESO blends' non-isothermal crystallization kinetics were examined using the Jeziorny [20] and the Liu, et al. [21].

2. Experimental

2.1. Materials

L-poly(lactic acid) (PLLA, Mw = 1.83 kg/mol) and D-poly(lactic acid) (PDLA, Mw = 0.79 kg/mol) were purchased from Shanghai Chemical Reagent Co., Ltd.; ESO was provided by Shandong Wushuang Chemical Group Co., Ltd., with a product purity greater than 99.99% and an epoxide value greater than 6.1; the solvent was analytical-grade chloroform ($CHCl_3$), supplied by Sinopharm Chemical Reagents Co., Ltd. (Beijing, China).

2.2. Sample Preparation

Neat PLLA and PDLA were continually dried for 48 hours at 70°C. PLLA and PDLA were combined at a 1:1 ratio with varying concentrations of ESO. In $CHCl_3$, the mixture was dissolved. After that, the mixture was agitated with a stirrer for six hours to dissolve it fully. A Petri plate was then filled with the solution, which was allowed to evaporate for about twenty-four hours at normal temperature. The collected samples were then vacuum-dried to a consistent weight. The blends of PLLA and PDLA that contained 0%, 8%, and 20% ESO were designated SC-PLA, SC-PLA-8ESO, and SC-PLA-20ESO.

2.3. Test and Characterization

Under a nitrogen flow rate of 19.8 mL/min, non-isothermal crystallization tests were performed on SC-PLA mixes with varying ESO levels using a differential scanning calorimetry (DSC) device (NETZSCH DSC204F1). Prior to isothermally maintaining the reweighed samples (≤8 mg) for 3 minutes, they were heated to 250 °C. After cooling the samples to 30 °C at various rates of 5, 10, 15, and 20 °C/min, they were reheated to 250 °C at a rate of 10 °C/min. DSC curves for the cooling process were plotted, and measurements were made of the peak temperature (T_c) and enthalpy (ΔH_c) during the cooling crystallization process.

3. Results and Discussion

3.1. Cooling Crystallization Process of SC-PLA-ESO Blends

The DSC curves of the SC-PLA-ESO blend chilled at rates of 5, 10, 15, and 20°C/min are displayed in Figure 1, and the parameters derived from the DSC curves are compiled in Table 1.

Edelweiss Applied Science and Technology
ISSN: 2576-8484
Vol. 9, No. 9: 1367-1376, 2025
DOI: 10.55214/2576-8484.v9i9.10135

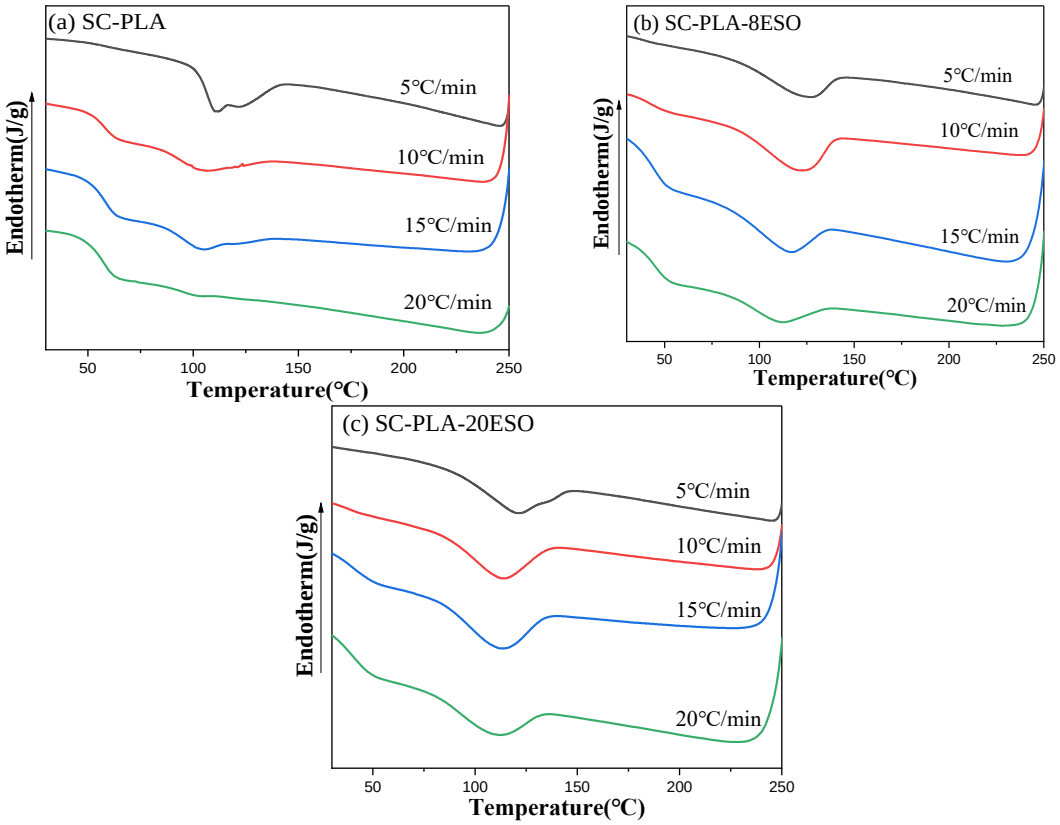

Figure 1.
DSC cooling curves at various cooling rates (marked on the curve).

As shown in Figure 1(a–c) and Table 1, the crystallization peak temperatures of SC-PLA, SC-PLA-8ESO, and SC-PLA-20ESO all decrease with increasing cooling rate. This is due to the temperature dependence of the phase transition process, as the blends require stronger undercooling to induce crystallization. Furthermore, the T_c values of the blends including ESO are noticeably greater than those of the neat SC-PLA blends at the same cooling rate, suggesting that ESO functions as a nucleating agent for crystallization, encouraging crystallization in the blends. Moreover, the crystallization enthalpy (ΔH_c) of every sample progressively drops as the cooling rate rises. This is because rapid sample cooling shortens diffusion times into the crystal lattice and decreases molecular chain mobility because molecular chain movement cannot keep up with the temperature drop.

Edelweiss Applied Science and Technology
ISSN: 2576-8484
Vol. 9, No. 9: 1367-1376, 2025
DOI: 10.55214/2576-8484.v9i9.10135

Table 1.
Cooling parameters at various cooling rates.

Samples	Cold crystallization process		
	Cooling rates (℃/min)	Temperature T_c(℃)	crystallization enthalpy ΔH_c (J/g)
SC-PLA	5	110.36	-39.06
	10	106.35	-8.35
	15	104.02	-5.52
	20	-	-
SC-PLA-8ESO	5	125.93	-27.53
	10	121.51	-20.82
	15	116.35	-8.46
	20	111.53	-7.05
SC-PLA-20ESO	5	120.52	-33.24
	10	113.50	-17.85
	15	111.77	-13.77
	20	110.36	-7.98

The relationship between relative crystallinity (X_T) and crystallization temperature (T) can be expressed as follows:

$$X_T = \int_{T_0}^{T} (\mathrm{d}H_c/\mathrm{d}T)\mathrm{d}T / \int_{T_o}^{T\infty} (\mathrm{d}H_c/\mathrm{d}T)\mathrm{d}T \qquad (1)$$

In this context, where T_0 and T_∞ stand for the beginning and ending crystallization temperatures, respectively. During an infinitesimal temperature range, the crystallization enthalpy emitted is represented by the dHc. X_T versus T is illustrated in Figure 2 (a–c). It can be observed that during the initial stage of crystallization, nucleation occurs relatively slowly, exhibiting a gradual progression. As crystallization enters the intermediate stage, crystal growth becomes the dominant trend, and crystallinity increases rapidly during this phase. However, as crystals continue to grow, the crystallization process gradually stabilizes in the later stages. This evolutionary process reflects the characteristics and changes of crystallization at different stages. The crystallization range of the blend is primarily concentrated between 90°C and 140°C. This specific temperature range is critical for the performance of polylactic acid materials, as it allows the molecular chains of the blend to arrange in an ordered manner, forming a stable crystalline structure, thereby enhancing the material's crystallinity and related properties.

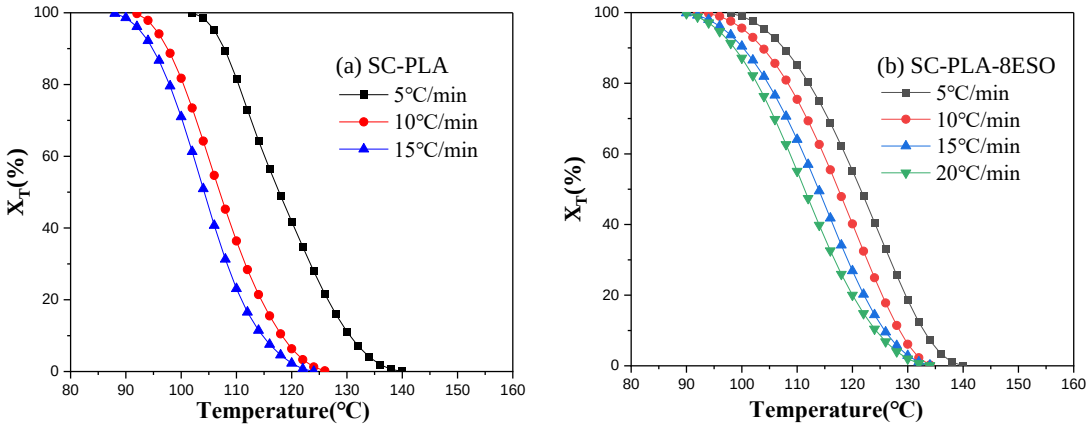

Edelweiss Applied Science and Technology
ISSN: 2576-8484
Vol. 9, No. 9: 1367-1376, 2025
DOI: 10.55214/2576-8484.v9i9.10135

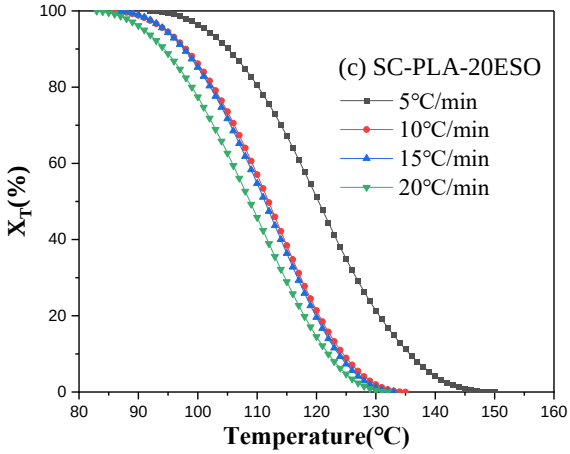

Figure 2.
Plots of relative crystallinity (X_T) versus crystallization temperature(T) at various cooling rates.

The following equation can be used to convert X_T data to X_t data:

$$X_t = (T_0 - T)/\Phi \qquad (2)$$

In this case, T refers to the temperature at crystallization time t, and Φ refers to the cooling rate, resulting in the curves shown in Figure 3 (a-c). A higher cooling rate results in a decrease in the crystallinity curve and the crystallization completion time. In the later stages of crystallization, the upward slope of the curve significantly slows down. This is due to the fact that when crystals get bigger, they collide with one another to form grain boundaries, which prevent and postpone additional crystal growth until the crystallization eventually flattens out and stops.

At the same cooling rate, as the ESO content increases, the crystallization time of the blend decreases. This phenomenon is primarily attributed to interactions between ESO and the PLA-based blend molecular chains. With higher ESO content, the mobility of the molecular chains in the blend improves, facilitating faster ordered arrangement during crystallization.

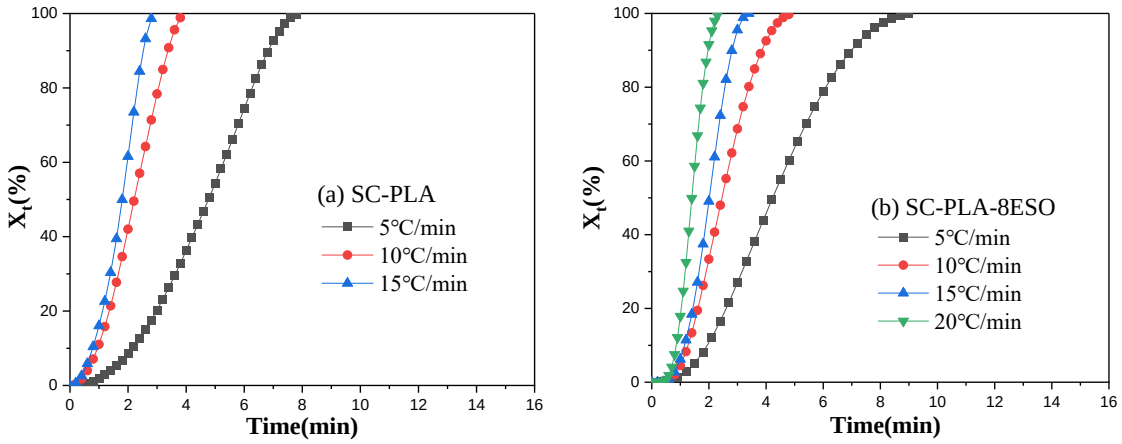

Edelweiss Applied Science and Technology
ISSN: 2576-8484
Vol. 9, No. 9: 1367-1376, 2025
DOI: 10.55214/2576-8484.v9i9.10135

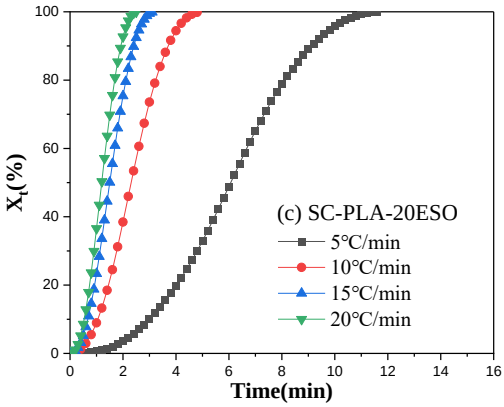

Figure 3.
Plots of relative crystallinity (X_t) versus crystallization time (t) at various cooling rates.

3.2. Jeziorny Method for Studying Non-Isothermal Crystallization Kinetics

The Avrami [22] is a kinetic equation that describes crystal nucleation and growth during the crystallization reaction. It is widely used in the study of polymer crystallization kinetics. The equation is expressed as follows:

$$\lg\left[-\ln\left(1-X(t)\right)\right] = n\lg\, t + \lg\, K \qquad (3)$$

In this equation, n is the Avrami exponent in non-isothermal crystallization, and K is the non-isothermal crystallization rate constant. To eliminate the influence of the cooling rate during the non-isothermal crystallization of polymers, Jeziorny proposed that the cooling rate (Φ) can be used to correct the rate constant K during the crystallization process.

$$\lg K_c = \lg K\, /\Phi \qquad (4)$$

Where K_c is the corrected crystallization rate constant and $t_{1/2}$ is the crystallization half-life:

$$t_{1/2} = (ln2/k_c)^{1/n} \qquad (5)$$

The linear fitting plots of the Avrami index n, K_c, and $t_{1/2}$ are displayed in Figure 4(a–c) and Table 2, along with the connection between log[-ln(1-Xt)] and logt for SC-PLA, SC-PLA-8ESO, and SC-PLA-20ESO at various cooling rates. The polymer's nucleation and growth mechanism are reflected in the n value. Compared to neat SC-PLA and SC-PLA with 20% ESO content, the n value for SC-PLA with 8% ESO content is greater, suggesting that the 8% ESO content has the greatest impact on the nucleation and growth mechanism of SC-PLA. The K_c value of SC-PLA-ESO rises with increasing cooling rate, suggesting that the polymer's crystallization rate is directly proportional to chilling rate. The linear component of the data was well-fitted, as indicated by the R^2 values of the linear regression coefficients for all samples being higher than 0.98.

Edelweiss Applied Science and Technology
ISSN: 2576-8484
Vol. 9, No. 9: 1367-1376, 2025
DOI: 10.55214/2576-8484.v9i9.10135

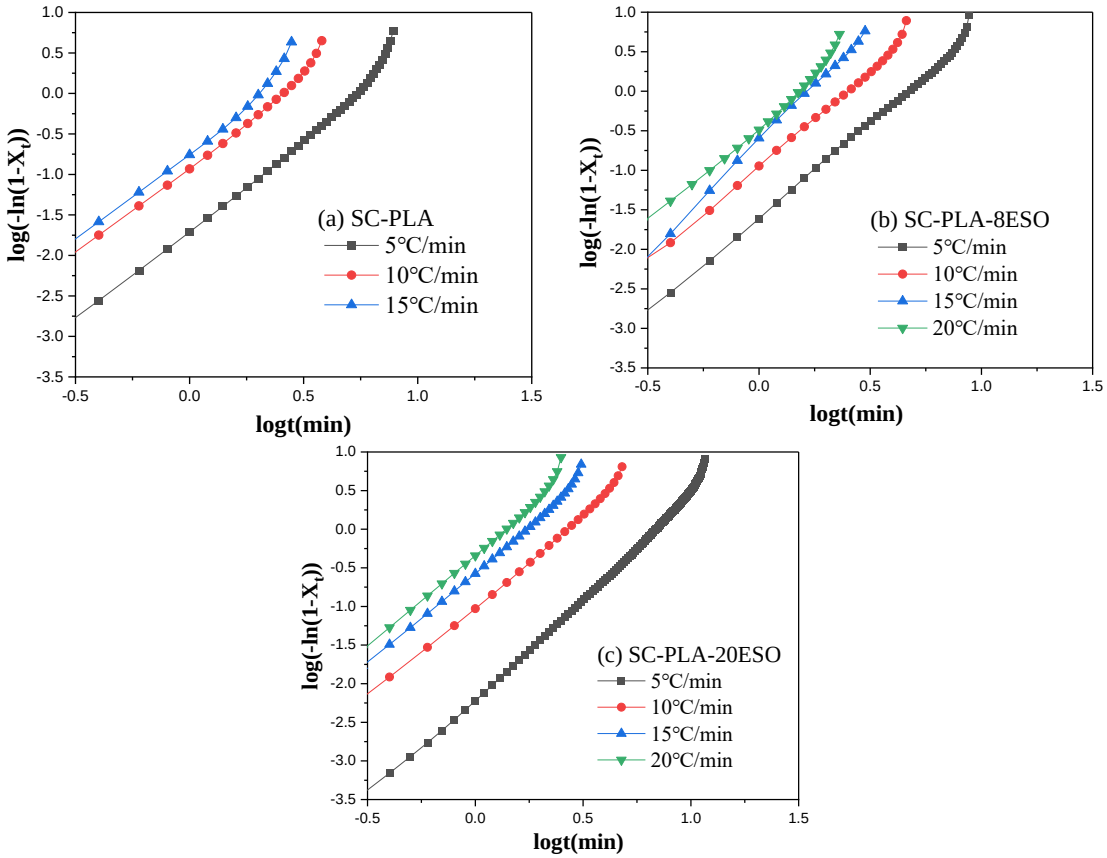

Figure 4.
Plots of log[-ln(1-X_t)] versus logt at various cooling rates.

Table 2.
Non-isothermal crystallization kinetics based on Jeziorny method.

Samples	Φ (℃/min)	*n*	K_c ($*10^2$)	$t_{1/2}$ (min)	R^2
SC-PLA	5	2.39	45.5	1.183	0.986 39
	10	2.27	81.47	0.931	0.989 78
	15	2.37	90.09	0.895	0.980 38
SC-PLA-8ESO	5	2.52	45.08	1.163	0.995 75
	10	2.41	80.72	0.939	0.993 74
	15	2.86	89.78	0.91	0.999 08
	20	2.44	95.5	0.877	0.988 89
SC-PLA-20ESO	5	2.44	36.59	1.274	0.994 33
	10	2.40	79.55	0.942	0.995 7
	15	2.38	92.12	0.887	0.995 02
	20	2.43	94.64	0.872	0.993 06

3.3. Mo Method for Studying Non-Isothermal Crystallization Kinetics

The following equation for non-isothermal crystallization processes is created by the Mo technique by combining the Avrami and Ozawa equations: Analysis of non-isothermal crystallization dynamics using the Mo method.

$$\log\Phi = \log F(T) - \alpha \log t \qquad (6)$$

Among these, F(T) indicates the cooling rate needed for the system to reach a specific relative crystallinity in a particular amount of time, and Φ stands for the cooling rate. The ratio of the Ozawa

Edelweiss Applied Science and Technology
ISSN: 2576-8484
Vol. 9, No. 9: 1367-1376, 2025
DOI: 10.55214/2576-8484.v9i9.10135

index m to the Avrami index n (n/m) is denoted by α. A set of well-fitting straight lines can be created by charting the relationship curve between logt and logΦ (Figure 5(a–c)). The parameters α and F(T), which were obtained from the slope and intercept of the straight lines, are listed in Table 3. Mo method combines the Avrami equation and the Ozawa [23] to design an equation for non-isothermal crystallization processes. It has been proven that the Mo method is well suited for studying non-isothermal crystallization kinetics.

As relative crystallinity rises, the F(T) value rises as well, suggesting that higher crystallinity must be attained in a given amount of time at a quicker cooling rate. Furthermore, the F(T) value of SC-PLA blends including ESO is lower than that of neat SC-PLA under the same relative crystallinity conditions, indicating that the blends' crystallization rate has been increased [24]. The α value, which falls between 0.81 and 1.32, shows that the Avrami index n and the Ozawa index m do, in fact, have a proportionate relationship. This suggests that the Mo approach can well characterize the non-isothermal crystallization process of polylactic acid and its blends.

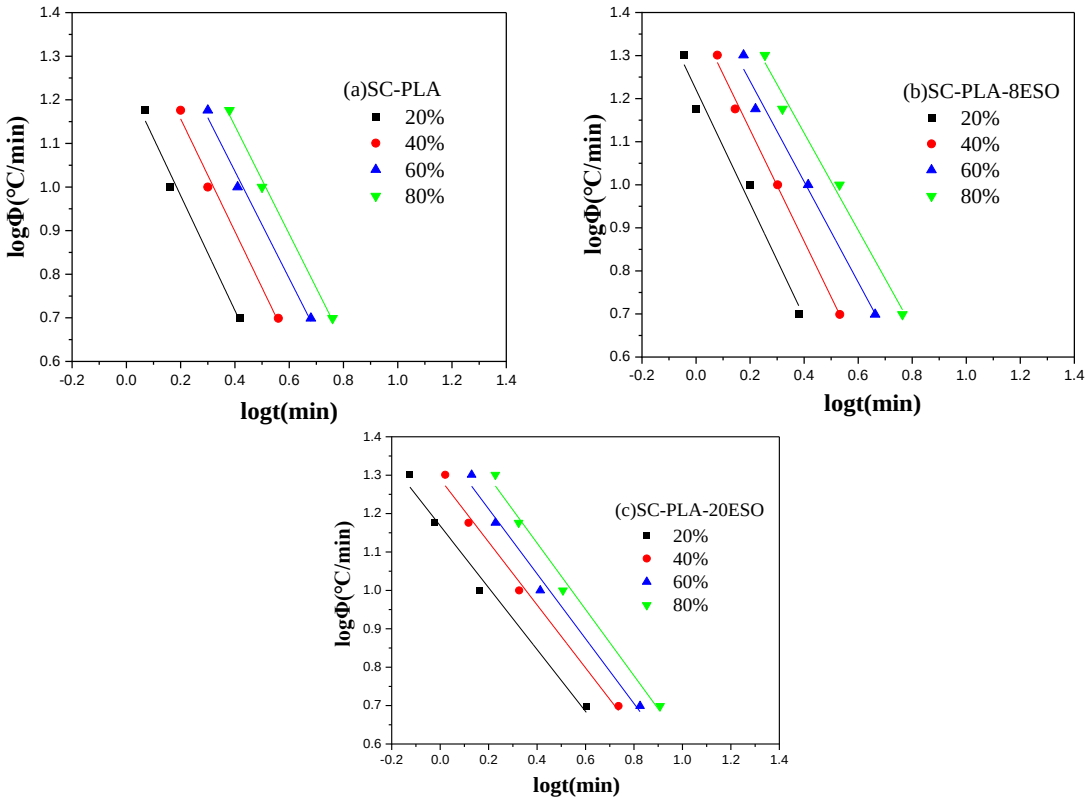

Figure 5.
Plots of logt versus logΦ at various relative crystallinity.

Edelweiss Applied Science and Technology
ISSN: 2576-8484
Vol. 9, No. 9: 1367-1376, 2025
DOI: 10.55214/2576-8484.v9i9.10135

Table 3.
Parameters of non-isothermal crystallization kinetics by the Mo method.

Samples	X(t)(%)	α	F(T)	R^2
SC-PLA	20	1.32	17.38	0.984 89
	40	1.29	25.70	0.989 83
	60	1.23	33.88	0.992 22
	80	1.24	43.65	0.996 47
SC-PLA-8ESO	20	1.32	16.60	0.976 66
	40	1.29	24.55	0.995 98
	60	1.17	29.51	0.986 01
	80	1.13	37.15	0.988 48
SC-PLA-20ESO	20	0.81	14.79	0.985 88
	40	0.82	19.50	0.991 23
	60	0.84	23.99	0.988 76
	80	0.86	29.51	0.989 34

4. Conclusions

The blend incorporating ESO had a T_c value that was much higher than that of the neat SC-PLA blend under the same cooling rate, as validated by DSC experiments with varying cooling rates. This suggests that ESO facilitates the blend's crystallization by acting as a nucleating agent. According to the Jezinory method, which was used to examine the crystallization process, the K_c value of SC-PLA-ESO grew as the cooling rate increased. This suggests that the polymer's crystallization rate is directly proportional to the cooling rate. The non-isothermal crystallization behavior of SC-PLA-ESO blends is well described by the Mo technique. The rise in the F(T) value of blends including ESO under the same relative crystallinity suggests that ESO speeds up the crystallization of PLA blends.

Funding:

The work was financially supported by the Scientific Research Fund of Hunan Provincial Education Department (24B0999)

Transparency:

The authors confirm that the manuscript is an honest, accurate, and transparent account of the study; that no vital features of the study have been omitted; and that any discrepancies from the study as planned have been explained. This study followed all ethical practices during writing.

References

[1] W. De-bao, Z. Yu-fu, L. Jia, Y. Duo, and L. Xing-yun, "Effects on the preservation of chilled mutton by using polylactic acid nanofiber films loaded with perillaldehyde," *Food and Machinery*, vol. 39, no. 7, pp. 131-136, 2023.

[2] O. Okolie *et al.*, "Bio-based sustainable polymers and materials: From processing to biodegradation," *Journal of Composites Science*, vol. 7, no. 6, p. 213, 2023. https://doi.org/10.3390/jcs7060213

[3] L. R. Carneiro da Silva, A. D. O. Rios, and R. M. Campomanes Santana, "Polymer blends of poly (lactic acid) and starch for the production of films applied in food packaging: A brief review," *Polymers from Renewable Resources*, vol. 14, no. 2, pp. 108-153, 2023. https://doi.org/10.1177/20412479231154924

[4] N. M. Ainali *et al.*, "Do poly (lactic acid) microplastics instigate a threat? A perception for their dynamic towards environmental pollution and toxicity," *Science of the Total Environment*, vol. 832, p. 155014, 2022. https://doi.org/10.1016/j.scitotenv.2022.155014

[5] T. P. Haider, C. Völker, J. Kramm, K. Landfester, and F. R. Wurm, "Plastics of the future? The impact of biodegradable polymers on the environment and on society," *Angewandte Chemie International Edition*, vol. 58, no. 1, pp. 50-62, 2019. https://doi.org/10.1002/anie.201805766

[6] N. Shekhar and A. Mondal, "Synthesis, properties, environmental degradation, processing, and applications of Polylactic Acid (PLA): An overview," *Polymer Bulletin*, vol. 81, pp. 11421-11457, 2024. https://doi.org/10.1007/s00289-024-05252-7

[7] F. Imani, R. Karimi-Soflou, I. Shabani, and A. Karkhaneh, "PLA electrospun nanofibers modified with polypyrrole-grafted gelatin as bioactive electroconductive scaffold," *Polymer*, vol. 218, p. 123487, 2021. https://doi.org/10.1016/j.polymer.2021.123487

[8] E. Piorkowska, Z. Kulinski, A. Galeski, and R. Masirek, "Plasticization of semicrystalline poly (L-lactide) with poly (propylene glycol)," *Polymer*, vol. 47, no. 20, pp. 7178-7188, 2006. https://doi.org/10.1016/j.polymer.2006.03.115

[9] H. Zhao and X. HU SP, "Structures and prop- erties of PBAT/PLA composites with chain extender," *Engineering Plastics Application*, vol. 49, no. 10, p. 131, 2021.

[10] X. Zhao, J. Liu, J. Li, X. Liang, W. Zhou, and S. Peng, "Strategies and techniques for improving heat resistance and mechanical performances of poly (lactic acid)(PLA) biodegradable materials," *International Journal of Biological Macromolecules*, vol. 218, pp. 115-134, 2022. https://doi.org/10.1016/j.ijbiomac.2022.07.091

[11] S. Marano, E. Laudadio, C. Minnelli, and P. Stipa, "Tailoring the barrier properties of PLA: A state-of-the-art review for food packaging applications," *Polymers*, vol. 14, no. 8, p. 1626, 2022. https://doi.org/10.3390/polym14081626

[12] W. Li, J. Shen, Y. Srithep, P. Worajittiphon, and S. J. Liu, "Effect of epoxidized natural rubber on the crystallization, thermal stability, and rheological behavior of polylactide stereocomplexes," *Polymers for Advanced Technologies*, vol. 36, no. 4, p. e70178, 2025. https://doi.org/10.1002/pat.70178

[13] X. Chen *et al.*, "Fully bio-based and supertough PLA blends via a novel interlocking strategy combining strong dipolar interactions and stereocomplexation," *Macromolecules*, vol. 55, no. 13, pp. 5864-5878, 2022. https://doi.org/10.1021/acs.macromol.2c00266

[14] W. Chen, S. Wang, W. Zhang, Y. Ke, Y.-l. Hong, and T. Miyoshi, "Molecular structural basis for stereocomplex formation of polylactide enantiomers in dilute solution," *ACS Macro Letters*, vol. 4, no. 11, pp. 1264-1267, 2015.

[15] P. Jia, Y. Zhou, L. Hu, C. Bo, and J. Zhou, "Application and progress of green plasticizers," *China Plast*, vol. 28, pp. 6-10, 2014.

[16] W. Li *et al.*, "Preferential formation of the stereocomplex crystals of poly (l-lactide) and poly (d-lactide) blend by epoxidized soybean oil under nonisothermal crystallization," *Polymers for Advanced Technologies*, vol. 35, no. 1, p. e6278, 2024. https://doi.org/10.1002/pat.6278

[17] Z. Ren *et al.*, "Multiscale interface design for toughened polylactic acid green composites," *ACS Sustainable Chemistry & Engineering*, vol. 12, no. 34, pp. 12763-12774, 2024. https://doi.org/10.1021/acssuschemeng.4c02321

[18] Z. Zhang, S. Huo, G. Ye, C. Wang, Q. Zhang, and Z. Liu, "Flame-retardant and tough poly (lactic acid) with well-preserved mechanical strength via reactive blending with bio-plasticizer and phosphorus derivative," *Materials Today Chemistry*, vol. 40, p. 102252, 2024. https://doi.org/10.1016/j.mtchem.2024.102252

[19] Q.-y. Ge and Q. Dou, "Preparation of supertough polylactide/polybutylene succinate/epoxidized soybean oil bio-blends by chain extension," *ACS Sustainable Chemistry & Engineering*, vol. 11, no. 26, pp. 9620-9629, 2023. https://doi.org/10.1021/acssuschemeng.3c01042

[20] A. Jeziorny, "Parameters characterizing the kinetics of the non-isothermal crystallization of poly (ethylene terephthalate) determined by DSC," *Polymer*, vol. 19, no. 10, pp. 1142-1144, 1978. https://doi.org/10.1016/0032-3861(78)90060-5

[21] T. Liu, Z. Mo, and H. Zhang, "Nonisothermal crystallization behavior of a novel poly (aryl ether ketone): PEDEKmK," *Journal of Applied Polymer Science*, vol. 67, no. 5, pp. 815-821, 1998. https://doi.org/10.1002/(SICI)1097-4628(19980131)67:5<815::AID-APP6>3.0.CO;2-W

[22] M. Avrami, "Kinetics of phase change. I General theory," *The Journal of Chemical Physics*, vol. 7, no. 12, pp. 1103-1112, 1939. https://doi.org/10.1063/1.1750380

[23] T. Ozawa, "Kinetics of non-isothermal crystallization," *Polymer*, vol. 12, no. 3, pp. 150-158, 1971. https://doi.org/10.1016/0032-3861(71)90041-3

[24] H. Huang, L. Gu, and Y. Ozaki, "Non-isothermal crystallization and thermal transitions of a biodegradable, partially hydrolyzed poly (vinyl alcohol)," *Polymer*, vol. 47, no. 11, pp. 3935-3945, 2006. https://doi.org/10.1016/j.polymer.2006.03.089

Edelweiss Applied Science and Technology
ISSN: 2576-8484
Vol. 9, No. 9: 1367-1376, 2025
DOI: 10.55214/2576-8484.v9i9.10135